Estimation of the Central Arterial Pressure Waveform and Beat-to-Beat Stroke Volume from Multiple Peripheral Arterial Pressure Waveforms

G Swamy, R Mukkamala

Michigan State University, East Lansing, MI, USA

Abstract

We introduce a new technique to estimate the clinically more relevant central arterial pressure (AP) waveform and relative beat-to-beat changes in stroke volume (SV) from multiple, less invasively measured peripheral AP waveforms distorted by wave reflections. The basic idea is to first reconstruct the central AP waveform by applying multi-channel blind system identification and to then estimate beat-to-beat proportional SV by fitting a Windkessel model to the reconstructed waveform in which wave distortion should be attenuated. We evaluated the technique in four swine in which two peripheral AP waveforms and gold standard central AP and SV were simultaneously measured during diverse hemodynamic interventions. We report an overall central AP error of 5.6% and an overall beat-to-beat SV error of 14.7%.

1. Introduction

As the arterial pressure (AP) wave traverses from the central aorta to the smaller, peripheral arteries, its contour becomes significantly distorted due to highly complex wave reflections in the distributed arterial tree [1]. For example, both the systolic pressure and pulse pressure usually become amplified, with the extent of the amplification dependent on the particular peripheral site and state of the arterial tree [2]. Thus, it is the systolic and diastolic pressures measured specifically in the central aorta that truly reflect cardiac afterload and perfusion [3]. Perhaps, as a result, central measurements of systolic pressure and pulse pressure have been shown to be superior in predicting patient outcome than corresponding measurements made in more peripheral arteries [4,5]. Moreover, central AP is not substantially complicated by the wave reflections [6,7]. Thus, the entire central AP waveform clearly reveals the cardiac ejection time through the dicrotic notch (which is usually obscured by wave phenomena in peripheral AP waveforms) [8] and may be fitted to a simple Windkessel model in order to accurately estimate other clinically important cardiovascular variables including relative beat-to-beat changes in stroke volume (SV) [6]. The measurement of the central AP waveform involves introducing a catheter into a peripheral artery and guiding the catheter against the flowing blood to the central aorta. However, placement of an aortic catheter is not commonly performed in clinical practice [3,9] because of the risk of blood clot formation and embolization.

On the other hand, related, but distorted, peripheral AP waveforms may be measured less invasively and more safely via placement of a catheter in a distal artery. Indeed, radial and femoral artery catheters are routinely placed in clinical practice [9]. Moreover, non-invasive methods are commercially available to continuously measure peripheral AP based on finger-cuff photo-plethysmography [10] and applanation tonometry [11]. Several techniques have therefore been recently introduced to derive the clinically more relevant central AP waveform from less invasively measured peripheral AP. Most of these techniques have involved 1) initially obtaining simultaneous measurements of central and peripheral AP waveforms in a group of subjects, 2) estimating a group-averaged transfer function relating the measured peripheral AP to the measured central AP, and 3) subsequently applying this generalized transfer function to peripheral AP measured from an individual subject in order to predict the unobserved central AP waveform [2,3,8,12]. The principal assumption underlying these techniques is that arterial tree properties are constant over all time and between all individuals. To soften this assumption, a few techniques have been more recently proposed towards partial individualization of the transfer function relating peripheral AP to central AP using a model-based [13,14].

It would be desirable to be able to estimate the central AP waveform from peripheral AP in a totally patient and time specific manner. One possible way to do so is with the recently developed, multi-channel blind system identification (MBSI) approach in which the outputs of a single input, multi-output system are analyzed so as to reconstruct the common input [15,16]. To our knowledge, the very recent study by McCombie et al. represents the first application of MBSI to the field of hemodynamic monitoring [17]. However, their study was specifically designed to estimate only the shape of the aortic flow waveform from peripheral AP measurements.

We have recently introduced a technique to estimate the central AP waveform from multiple peripheral AP waveforms based on a standard MBSI method [18]. Here, we present an improved technique to estimate the central AP waveform as well as relative beat-to-beat changes in SV from multiple peripheral AP waveforms based on a new MBSI method and Windkessel modeling. We then demonstrate the validity of the technique using four previously collected swine datasets [19] in which femoral and radial AP waveforms and highly invasive, gold standard central AP and SV were simultaneously measured during various hemodynamic interventions.

2. The technique

Our technique applies a novel MBSI method to two or more peripheral AP waveforms to reconstruct the central AP waveform and then employs a Windkessel model to estimate relative beat-to-beat changes in SV from the reconstructed waveform. The technique is specifically implemented in the four steps as follows.

First, m (>1) measured peripheral AP waveforms ($p_{pi}(t)$, $1 \le i \le m$) are modeled as individual outputs of m distinct channels driven by the common central AP input ($p_{ca}(t)$) as shown in Figure 1. Each of the channels coupling the common input to each distinct output characterizes the dynamic properties of a different arterial tree path. The main assumption underlying the model is that the channels may be well characterized by coprime finite impulse responses (FIRs; $h_i(t)$, $1 \le i \le m$) over each one-minute interval of analysis (see below) [15,16]. Note that, over such short time intervals, the arterial tree is usually operating in near steady-state conditions thereby supporting the implicit linearity and time-invariance assumptions (see [17] and references therein). Moreover, since AP waveforms from distinct arterial sites only differ significantly over short time scales [7,19]. The FIR assumption is also well justified.

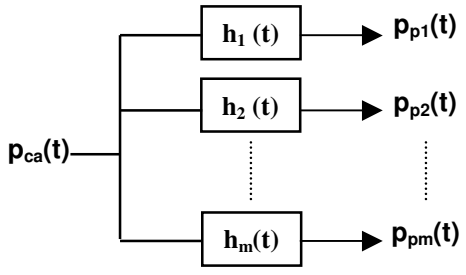

Figure 1. Single input, multi-output model upon which the reconstruction of the central AP waveform from multiple peripheral AP waveforms is based.

Then, the m FIRs are estimated from the m measured peripheral AP waveforms with a new MBSI method that we have recently developed. More specifically, the method is based on the following standard cross relations between pairs of measured outputs:

$$\sum_{k=0}^{L-1} h_j(k)\, y_i(t-k) - \sum_{k=0}^{L-1} h_i(k)\, y_j(t-k) = e_{ij}(t), \qquad 1 \le i \ne j \le m, \quad (1)$$

where $e_{ij}(t)$ accounts for measurement and/or modeling error, and L is the maximum duration or order of the m FIRS [15,16]. As suggested in [16], L is determined based on the number of significant singular values of the matrix formed by stacking each time instance of Eq. (1), one on top of the other, with an order that is expected to encompass the true order. To reduce the number of parameters to be estimated so as to decrease the error variance, the m FIRs are compactly represented with damped sinusoidal basis functions as follows:

$$h_i(t) = \sum_{k=1}^{n} \lambda^t (a_{ik} \cos(\omega_{ik} t) + b_{ik} \sin(\omega_{ik} t)), \qquad 1 \le i \le m, \quad (2)$$

where $\{\lambda, a_{ik}, b_{ik}, \omega_{ik}\}$ are unknown parameters, and n is the number of basis functions. The parameter λ is set equal to exp(-L/3). Then, for fixed n, the remaining parameters are uniquely estimated by substitution of Eq. (2) into Eq. (1) followed by least squares minimization of $e_{ij}(t)$ for $1 \le i \ne j \le m$ with the constraint that one FIR has unity gain. This constraint is justified, as the paths between the aorta and peripheral arteries offer very little resistance to blood flow due to Poiseuille's law [7]. The optimization here is specifically achieved by allowing the parameters $\{\omega_{ik}\}$ to take on only discrete values according to the Fourier Series (i.e., $2\pi l/L$, where $l=0,1,\ldots,(L-1)/2$) and estimating the parameters $\{a_{ik}, b_{ik}\}$ for each $\{\omega_{ik}\}$ using the closed-form linear least squares solution. The value of n is determined by starting with a single basis function and then adding one basis function at a time until the energy of $e_{ij}(t)$ for $1 \le i \ne j \le m$ no longer significantly decreases.

Next, the common central AP waveform input is reconstructed from the m estimated FIRs and measured peripheral AP waveforms via multi-channel least squares deconvolution. This procedure is specifically implemented with the closed-form linear least squares solution as described in [15].

Finally, relative beat-to-beat changes in SV are estimated from the reconstructed central AP waveform based on the Windkessel model of Figure 2a accounting for the nearly constant arterial compliance (C_a) [6,19] and the total peripheral resistance (R_a). That is, as described in [6], proportional beat-to-beat SV is calculated from the reconstructed central AP waveform according to the following equation governing the model:

$$SV \propto p_{ca}(t_{es}) - p_{ca}(t_{bs}) + \frac{1}{\tau}\int_{t_{bs}}^{t_{es}} p_{ca}(t)dt \ , \qquad (3)$$

where t_{es} and t_{bs} are defined in Figure 2b, and $\tau=R_aC_a$ is estimated by exponential fitting to each diastolic interval of the reconstructed waveform as shown in Figure 2b.

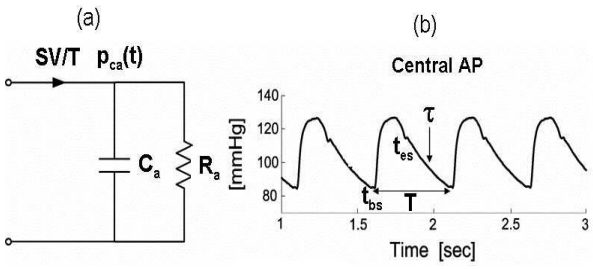

Figure 2. (a) Windkessel model representation of the reconstructed central AP waveform. (b) Determination of $\tau=R_aC_a$ and thus proportional SV (see Eq. (3)) from each beat of the reconstructed waveform based on the windkessel model.

3. Experimental evaluation

3.1. Hemodynamic data

The hemodynamic data utilized here to experimentally evaluate the technique were originally collected to address different specific aims, and the materials and methods are presented in detail elsewhere [19]. We briefly describe the experimental procedures below.

Four swine (30-34 kg) were studied under general anesthesia as follows. Catheters were inserted in the femoral artery for femoral AP, an artery as distal as possible to the brachial artery for radial AP, and the descending aorta via the opposite femoral artery for gold standard reference central AP. A midline sternotomy was performed, and an ultrasonic aortic flow probe was placed around the aortic root for gold standard reference beat-to-beat SV. The measurements were then recorded over the course of 75 to 150 minutes during various rates of infusion of dobutamine, isoproterenol, esmolol, phenylephrine, nitroglycerin, acetylcholine, volume, and/or progressive hemorrhage in order to vary the hemodynamic conditions over a wide range (see Table).

3.2. Data analysis

The technique was applied to all one-minute non-overlapping intervals of the femoral and radial AP waveforms (sampled at 50 Hz) in the four swine datasets. The resulting beat-to-beat proportional SV estimates were then scaled to have the same mean value as the aortic flow probe SV in each animal. Finally, the root-mean-squared-normalized-error (RMSNE) between each of the estimated and gold standard reference hemodynamic variables was computed as a metric for comparison.

4. Results

The Table summarizes the results of the experimental evaluation of the technique. The overall RMSNE of the estimated central AP waveforms was 5.6%. For comparison, the average overall RMSNE between the measured peripheral and central AP waveforms was 16.4%. Thus, the technique was effectively able to reduce the wave distortion in the peripheral AP waveforms by 67%. The overall error of the estimated beat-to-beat SV from the reconstructed central AP waveform was 14.7%. Figure 3a illustrates an example of the significant differences between the peripheral AP waveforms (short-dash and long-dash) and the measured central AP waveform (solid), while Figure 3b shows the resulting central AP waveform estimated from these peripheral AP waveforms (dash). Figure 4 provides a visual illustration of the close agreement between the estimated and calibrated beat-to-beat SV and the gold standard reference aortic flow probe measurements.

Table. Summary of the experimental evaluation of the technique.

ANIMAL	MAP RANGE [MMHG]	SV RANGE [ML]	CAP RMSNE [%]	PAP RMSNE [%]	SV RMSNE [%]
1	54 - 136	16 - 52	4.7	15.5	11.3
2	58 - 117	12 - 50	6.2	16.0	16.4
3	45 - 114	16 - 47	5.6	15.6	13.8
4	48 - 119	8 - 47	5.7	17.8	15.5
TOTAL	45 - 136	8 - 52	5.6	16.4	14.7

MAP is mean AP; CAP, central AP; and PAP, peripheral AP. See text for other abbreviations.

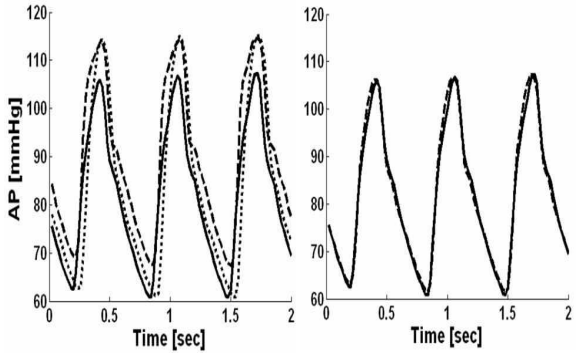

Figure 3. (a) Example segments of measured central AP (solid), femoral AP (long-dash), and radial AP (short-

dash) waveforms from one swine dataset. (b) Example segments of the resulting estimated (dash) and measured (solid) central AP waveforms.

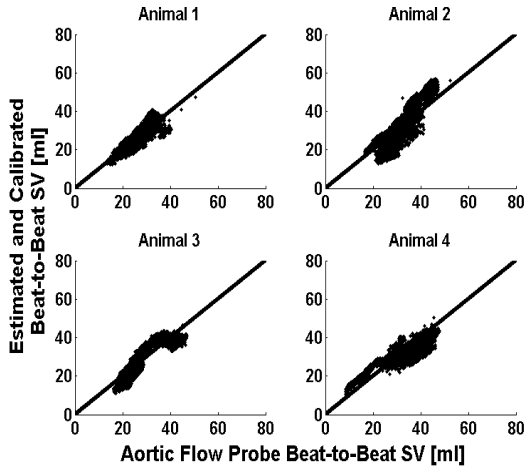

Figure 4. Beat-to-beat SV estimated (and calibrated) from the reconstructed central AP waveforms versus reference aortic flow probe SV for all four swine datasets.

5. Summary and conclusion

In summary, we have introduced a novel technique to estimate the clinically more relevant central AP waveform and relative beat-to-beat changes in SV from multiple, less invasively measured peripheral AP waveforms. We have applied the technique to femoral and radial AP waveforms from four swine over a wide hemodynamic range, and our results show excellent agreement with highly invasive, gold standard reference measurements. Potential applications of the technique include critical care monitoring with respect to invasive catheter systems as well as emergency and home monitoring with respect to non-invasive AP transducers.

Acknowledgements

This work was supported by the NIBIB Grant EB-004444 and an award from the AHA.

References

[1] O'Rourke MF, Yaginuma T. Wave reflections and the arterial pulse. Arch. Intern. Med 1984;144 :366-371, 1984.

[2] Soderstrom S, Nyberg G, O'Rourke MF, Sellgren J, Ponten J. Can a clinically useful aortic pressure wave be derived from a radial pressure wave? Br. J. Anaesth 2002;88:481-488.

[3] Chen CH, Nevo E, Fetics B, Pak PH, Yin FC, Maughan FL, Kass DA. Estimation of central aortic pressure waveform by mathematical transformation of radial tonometry pressure. Validation of generalized transfer function. Circulation 1997;95:1827-1836

[4] Safar ME, Blacher J, Pannier B, Guerin AP, Marchais SJ, Guyonvarc'h P, London GM. Central pulse pressure and mortality in end-stage renal disease. Hypertension 2002; 39:735-738

[5] Waddell TK, Dart AM, Medley TL, Cameron JD, Kingwell BA. Carotid pressure is a better predictor of coronary artery disease severity than brachial pressure. Hypertension 2001;38:927-931.

[6] Bourgeois MJ, Gilbert BK, Bernuth GV, Wood EH. Continuous determination of beat-to-beat stroke volume from aortic pressure pulses in the dog. Circ. Res. 1976;39:15-24.

[7] Noordergraaf A. Circulatory System Dynamics 1978. New York: Academic Press.

[8] Fetics B, Nevo E, Chen CH, and Kass DA. Parametric model derivation of transfer function for noninvasive estimation of aortic pressure by radial tonometry. IEEE Trans. Biomed. Eng. 1999;46:698-706.

[9] Marino PL. The ICU Book 1998. Baltimore: Lippincott Williams & Wilkins, 1998.

[10] Imholz BPM, Wieling W, Montfrans GAV, Wesseling KH. Fifteen years experience with finger arterial pressure monitoring: assessment of the technology. Cardiovasc. Res. 1998;38:605-616.

[11] Kenner T. ABP and its measurement. Basic Res. Cardiol. 1988;83:107-121.

[12] Karamanoglu M, O'Rourke MF, Avolio AP, Kelly RP. An analysis of the relationship between central aortic and peripheral upper limb pressure waves in man. Eur. Heart J. 1993;14:160-167.

[13] Karamanoglu M, Feneley MP. On-line synthesis of the human ascending aortic pressure pulse from the finger pulse. Hypertension 1997;30:1416-1424.

[14] Sugimachi M, Shishido T, Miyatake K, Sunagawa K. A new model-based method of reconstructing central aortic pressure from peripheral arterial pressure. Jpn. J. Physiol. 2001;51:217-222.

[15] Abed-Meraim K, Qiu W, Hua Y. Blind system identification. Proc. of IEEE 1997;85:1310-1332.

[16] Xu G, Liu H, Tong L, Kailath T. A least-squares approach to blind channel identification. IEEE Trans. Signal Processing 1995;43:2982-2993.

[17] McCombie DB, Reisner AT, Asada HH. Laguerre-model blind system identification: cardiovascular dynamics estimated from multiple peripheral circulatory signals. IEEE Trans. Biomed. Eng. 2005;52:1889-1901.

[18] Swamy G, Ling Q, Li T, Mukkamala R. Blind identification of the central aortic pressure waveform from multiple peripheral arterial pressure waveforms. Proc. 28th IEEE EMBS Conf. 2006;1:1822-1825.

[19] Mukkamala R, Reisner AT, Hojman HM, Mark RG, Cohen R. Continuous cardiac output monitoring by peripheral blood pressure waveform analysis. IEEE Trans. Biomed. Eng. 2006;53:459-467.

Address for correspondence

Ramakrishna Mukkamala
2120 Engineering Building
East Lansing, MI 48824
rama@egr.msu.edu